ISSN 1819-7140, Russian Journal of Pacific Geology, 2024, Vol. 18, Suppl. 2, pp. S229–S242. © Pleiades Publishing, Ltd., 2024.
Russian Text © The Author(s), 2024, published in Vestnik Kamchatskoy Regional'noy Assotsiatsii "Uchebno-Nauchnyy Tsentr". Seriya: Nauki o Zemle, 2024, No. 2(62), pp. 49–65.

Ivan Grozny Volcano (Iturup Island, Kuril Islands): Composition of Erupted Materials and Modern Activity

R. V. Zharkov[a], *, O. V. Bergal-Kuvikas[b, c], A. V. Degterev[a], F. A. Romanyuk[a], and S. E. Borisovsky[c]

[a] *Institute of Marine Geology and Geophysics, Far Eastern Branch, Russian Academy of Sciences, Yuzhno-Sakhalinsk, 693022 Russia*

[b] *Institute of Volcanology and Seismology, Far Eastern Branch, Russian Academy of Sciences, Petropavlovsk-Kamchatsky, 683006 Russia*

[c] *Institute of Geology of Ore Deposit, Petrography, Mineralogy and Geochemistry, Russian Academy of Sciences, Moscow, 119017 Russia*

**e-mail: rafael_zharkov@mail.ru*

Received February 6, 2023; revised May 10, 2024; accepted June 25, 2024

Abstract—The paper summarizes data on the historical activity of Ivan Grozny volcano (Iturup Island, Kuril Islands), including the results of original studies of sulfur hydrothermal and eruptive activities of the volcano since 2004. New chemical data on the volcanic edifice rocks and pyroclastics of the last explosive eruption in 2012–2013 are presented. The composition of the volcanic edifice rocks varies from andesites to dacitic andesites (58.16–61.42 wt % SiO_2) of the medium potassium series (0.93–1.14 wt % K_2O). Pyroclastics from the 2012–2013 explosive eruption chemically correspond to andesites (57.20–59.54 wt % SiO_2) with moderate potassium contents (0.95–1.05 wt % K_2O). According to microprobe studies, glasses have much more felsic compositions. The values obtained are similar to the geochemical compositions of the products of the 1973 and 1989 eruptions. Taking into account the dominant wind regime in central Iturup Island, the hazard from ashfalls from future eruptions of Ivan Grozny volcano is estimated, indicating the predominant ash spread in the northwestern, western, and southwestern directions.

Keywords: Kuril Islands, volcano, Ivan Grozny, eruption, pyroclastics, volcanic hazard

DOI: 10.1134/S1819714024700532

INTRODUCTION

Iturup Island belongs to the Southern Kuril Islands (Fig. 1a) and comprises nine volcanoes, which were active in historical time (Fig. 1b). Ivan Grozny volcano (true altitude is 1159 m) is located in the central part of Iturup Island (Fig. 1c) and can be considered as the most active volcano of this island. Its activity has been known only since the second half of 20th century: 1964–1965, 1967–1968, 1970–1973, 1989, and 2012–2013 (Abdurakhmanov et al., 1990; Zharkov and Kozlov, 2013), but in total, it exceeded the number of eruptions of other active volcanoes of Iturup Island for the same period. All historical eruptions of Ivan Grozny volcano were explosive but relatively weak, and the altitude of ash emissions did not exceed 3 km above sea level (Abdurakhmanov et al., 1990; Zharkov and Kozlov, 2013). The history of the eruptive activity of Ivan Grozny volcano at present has not been studied, but the morphology of its complex volcanic edifice suggests relatively recent (thousands of years ago) powerful eruptions in the volcanic life. Since Ivan Grozny volcano is located in the most populated and economically developed part of Iturup Island, the assessment of its volcanic hazard is great importance. All settlements of the island and main infrastructural objects, including fishery enterprises, Kurilsk Harbor in the village of Kitovoe, Yasny Airport, GeoTPP Okeanskaya (conserved since 2014 to present), and the Zharkie Vody and Vanochki thermal complexes in the Kipyashchaya River valley, restricted to a radius of 33 km from the volcano (Fig. 1c). During explosive eruptions, volcanic ash also presents a serious hazard not only to the population and terrestrial infrastructural objects, but also for local and international airlines passing along the Kuril Island Arc. At present, monitoring of the activity of Ivan Grozny volcano is based on satellite data and nonsystematic visual observations, but terrestrial instrumental observation base of the volcano state (seismic stations, GPS/TILLT-stations, and others) is absent. Therefore, any new data that allow to better characterize the activity and composition of this poorly accessible volcano are very valuable for future studies and assessment of the volcanic hazard of the region.

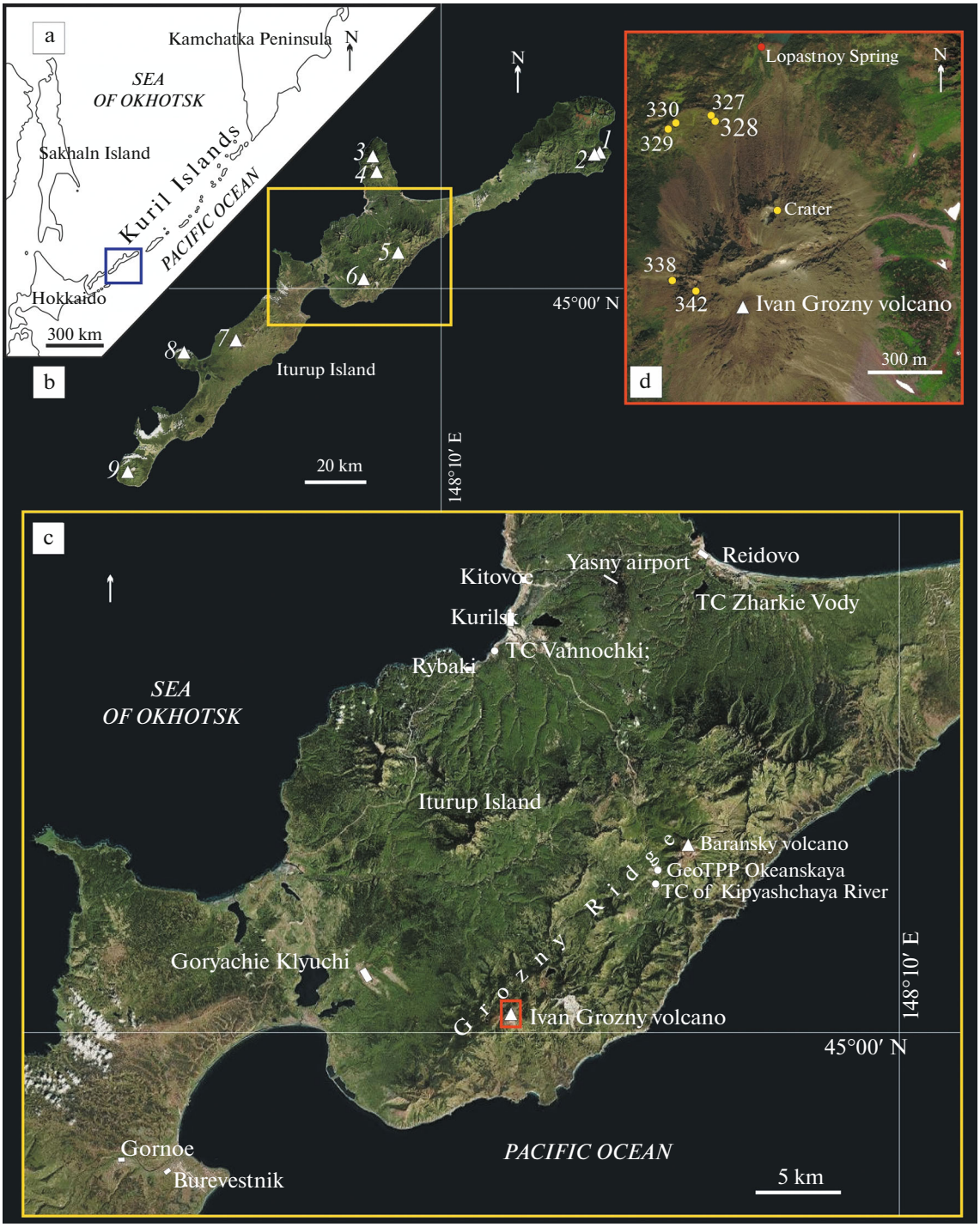

Fig. 1. Location scheme of Kuril Islands (a); active volcanoes of Iturup Island (b): (*1*) Kudryavy volcano, (*2*) Menshiy Brat volcano, (*3*) Chirip volcano, (*4*) Bogdan Khmelnitsky volcano, (*5*) Baransky volcano, (*6*) Ivan Grozny volcano, (*7*) Stokap volcano, (*8*) Atsonupuri volcano, (*9*) Berutarube volcano; geographical location of Ivan Grozny volcano, settlements and infrastructure facilities in central part of Iturup Island (c): TC—thermal complex, GeoTPP—geothermal power plant, sampling locality scheme in 2013 on slopes of Ivan Grozny volcano (d): yellow circles are eruption materials; red circles are hydrothermal vents of Lopastnoy spring.

The purpose of this publication is to generalize all available data on the historical activity of Ivan Grozny volcano, supplementing them with the results of our studies, including actual data on solfataric-hydrothermal activity, eruptions, and petrochemistry of rocks collected during field work in 2013 (Fig. 1d).

MATERIALS AND METHODS

The majority of the materials presented in this publication were obtained during 2012–2013 field work on Iturup Island, aimed at studying the thermal waters in the central part of the island and describing the consequences of the eruption of Ivan Grozny volcano (Zharkov, 2014).

Analytical studies on determining the concentrations of major and trace elements in whole-rock samples of volcanic rocks and local microprobe analysis of volcanic glasses were carried out at the Collective Use Center of the Institute of Geology of Ore Deposits, Petrography, Mineralogy, and Geochemistry, Russian Academy of Sciences (Moscow). Major oxides were measured by X-ray fluorescence (XRF) on an Axios mAX Advanced (PANalytical, Netherlands) wave-dispersive vacuum sequential spectrometer. The spectrometer is equipped with a 4-kW X-ray tube with Rh anode. The maximum voltage in the tube is 60 kV and the maximum anode current is 160 mA. Analysis of major components was performed using technique NSAM VIMS 439-RS (2010). To study the chemical composition using this technique, powdered samples were fused into glasslike disks by induction heating of an annealed sample with lithium borate at 1200°C. Standard samples of the US Geological Survey (USGS) were used as references. The obtained values of international standards correspond to the accepted measurement errors according to technique NSAM VIMS 439-RS (2010). The concentrations of trace elements were determined by inductively-coupled plasma mass spectrometry (ICP-MS) on an NEXION 2000C (United States) spectrometer. The quality of the measurement and sample preparation was controlled by the reference rock standards of the US Geological Survey (USGS): andesite AGV-2 and rhyolite RGM-2. Obtained values of the international standards correspond to the accepted errors according to the measurement technique NSAM No. 501-MS (2011). Mafic and intermediate rocks were prepared by the acid decomposition using technique (Bychkova et al., 2017). The glasses were analyzed on an JXA-8200 JEOL electron microprobe. The microprobe is equipped with a five-wave dispersion energy-dispersion spectrometer (EDS). The working voltage was 20 kV with a beam current of 10 nA. The beam diameter was widened to 6 μm. The peak and background counting times for all elements were 10 and 5 s. Si, Al, Mg, and Na were measured with a TAP crystal; Ca, K, Ti, P were measured with a PET crystal; Fe and Mn, with a LIF crystal. The reference samples were certified in-house standards: sanidine B-19 (for K, Al, Si), chkalovite $Na_2BeSi_2O_6$ (for Na), aegirine C-38 (for Fe, Na), anorthite K-2-Y (for Ca, Al), spessartine ABR (for Mn, Al), shorlomite C-68 (for Ti), olivine B-14 (for Mg), and $DyPO_4$ (for P). The studied samples were sputtered with carbon film around 200 angstrom thick to allow the charge compensation. Data reduction was performed using the internal ZAF matrix correction of JEOL.

The ash ejected by the August 18, 2012 explosion was analyzed at the Laboratory of the Analytical Center, Far East Geological Institute, Far Eastern Branch, Russian Academy of Sciences (Vladivostok); principal investigator N.V. Zarubina; analysts V.N. Kaminskaya, V.N. Zalevskaya, G.A. Gorbach, E.A. Tkalina, N.V. Khrukalo, and Yu.M. Ivanova. The H_2O and SiO_2 contents were determined gravimetrically; other elements were analyzed by the inductively-coupled plasma atomic emission spectrometry on an iCAP 6500 Duo spectrometer (Thermo Scientific Corporation, United States). Samples were prepared for instrumental analysis using open acid digestion ($HNO_3 + HClO_4 + HF$).

The volcanic (ash) hazard was assessed using database, which includes the diagrams and tables of wind regime (Mastin, 2017) constructed for each active volcano from catalogue (Siebert et al., 2010). The database is underlain by the meteorological model NCEP/NCAR Reanalysis 1 (Kalnay et al., 1996), which uses data array of regional meteostations and results of numerical modeling of weather during historical time. Data on the wind velocity and direction for each volcano were obtained by the linear interpolation for period from January 1, 1990 to December 28, 2009 and calculated for two values per a day (00:00 and 12:00 UTC). All these data are illustrated by diagrams, which were grouped based on the periods (January–March, April–June, July–September, October–December) and the emission altitude above sea level: 0–5, 5–11, 11–16, 16–24, and 24–40 km.

Schematic maps were made using satellite images from SAS. Planet 200606.10075 Stadle, © 2022 CNES/Airbus and © 2022 Maxar Technologies from Google Earth Pro, in the CorelDRAW Graphics Suite X8.

RESULTS AND DISCUSSION

The active Ivan Grozny volcano is located in the southwestern part of the volcanic Grozny Ridge (Fig. 1c), which also includes active Baransky volcano, as well as the Tebenkov, Machekha, and other volcanoes that dormant in the historical period (Fig. 2). This volcano was named after the Russian

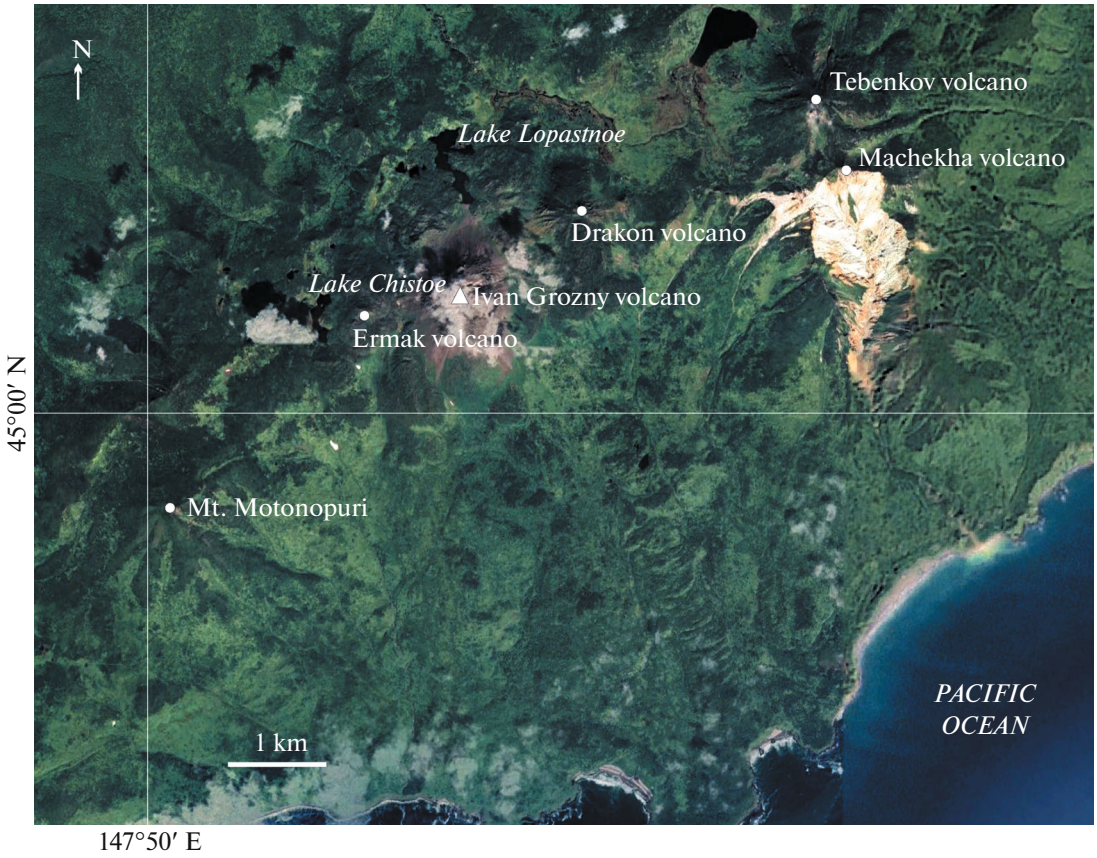

Fig. 2. Location of Ivan Grozny volcano and neighboring volcanoes inactive during historical period (Grozny Ridge, Iturup Island).

Tsar Ivan (Ioann) IV Vasil'evich Grozny (1530–1584) (Gal'tsev-Bezyuk, 1992).

The main details of the geological structure and morphology of Ivan Grozny volcano, as most of active volcanoes of the Kuril Island Arc, were established by Gorshkov (1976), who determined that the volcano corresponds to the Somma–Vesuvius type and is complicated by several parasitic edifices. In addition, he distinguished the caldera depression and numerous volcanic edifices of different age within it. The somma fragments representing the highly eroded small ridges have been preserved over the entire perimeter except for the southeastern sector; the crest of the caldera is almost completely destructed and traced only in the west and northwest, reaching altitudes 700–750 m above sea level, and its diameter is 3–3.5 km (Gorshkov, 1970). According to (Abdurakhmanov et al., 1990; Fedorchenko et al., 1989), the ancient volcanic edifice has an Early–Middle Pleistocene age, while the Middle–Upper Pleistocene rocks within this massif include Mt. Motonopuri and preserved part of the gentle cone crown by a wide crater with the effusive Ermak dome (Fig. 3). Lava-jammed Lake Chistoe is located in the crater between the Ermak dome and inner slope (Fig. 2). The youngest (Late Pleistocene–Holocene) rocks making up the complex Ivan Grozny volcanic massif are attributed to the Ermak, Ivan Grozny, and Drakon domes, which are merged at their bases and together with numerous small volcanic edifaces form an NE-trending chain (Abdurakhmanov et al., 1990). The modern extrusive Ivan Grozny dome has a complex structure and reaches an altitude around 500 m relative to lava-jammed Lake Lopastnoe. A detailed description of the dome morphology is given in (Gorshkov, 1970; Zharkov, 2013, 2014; Korsunskaya, 1958; Semakin et al., 2000[1]). It consists of three large blocks complicated by explosive funnels; agglomerate mantle almost everywhere descends to the foot (Fig. 1d), locally short lava flows on the slopes emerge from beneath it, indicating that (Gorshkov, 1970) the dome grew in the crater of the older central cone. The flows reach the caldera wall in the northern

[1] V. P. Semakin, G. S. Shteynberg, A. V. Rybin, et al., Volcanic Zoning and Control of the State of the Volcanoes of the Kuril Island Arc. Report on Research Activity. (IMGiG DVO RAN, Yuzhno-Sakhalinsk, 2000), no. 3166 (in Russian)].

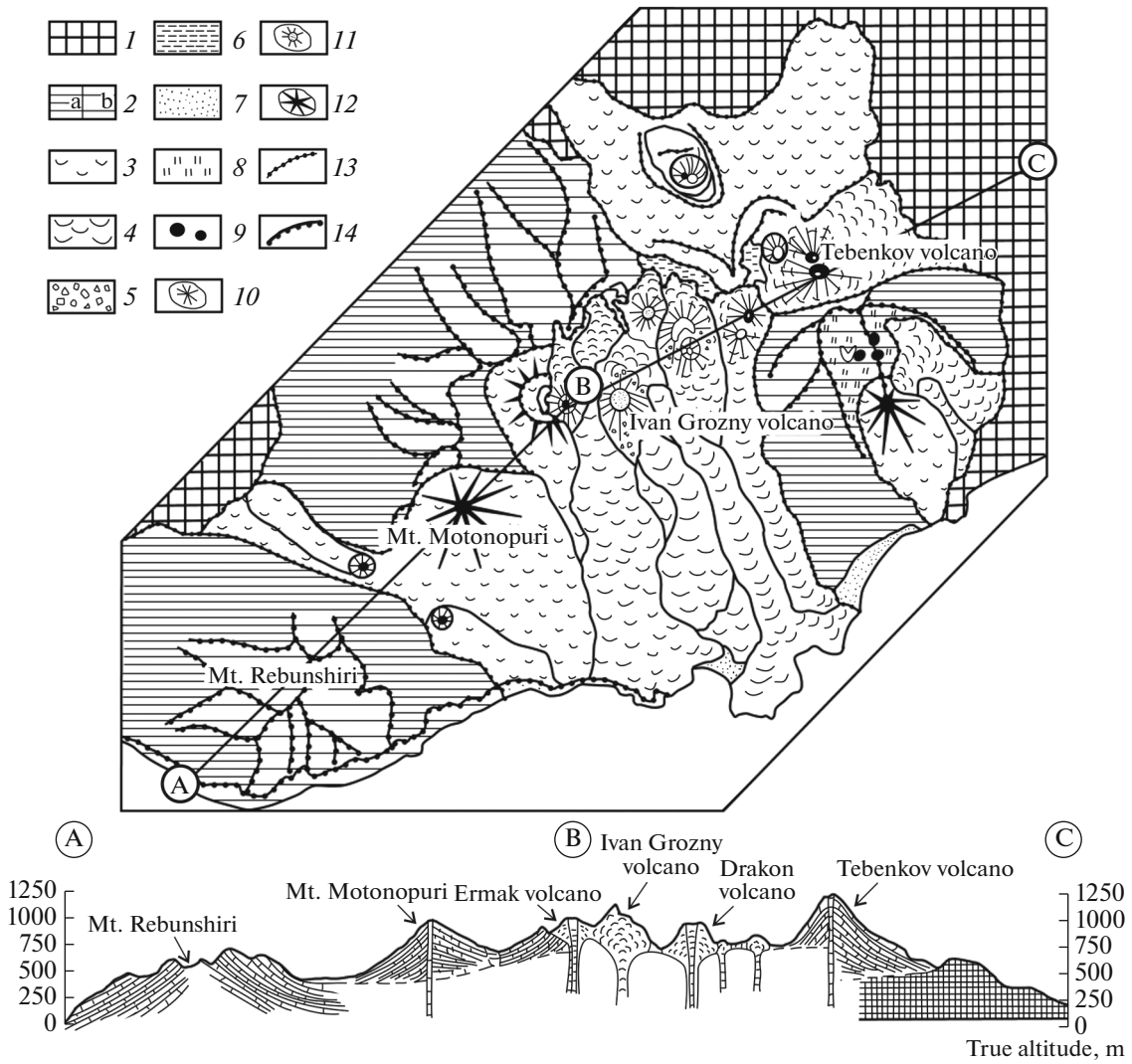

Fig. 3. Geological scheme of Grozny Ridge (according to (Fedorchenko et al., 1989)): (*1*) Neogene basement; (*2*) relicts of Early–Middle Pleistocene stratovolcanoes: (a) areas of primary slopes, (b) exposed by erosion, inner parts of cones; (*3*) Late Pleistocene volcanic rocks; (*4*) Holocene volcanic rocks; (*5*) agglomerate mantle of extrusive domes; (*6*) Holocene lacustrine sediments; (*7*) modern sea beach; (*8*) hydrothermally altered rocks; (*9*) exposed vents (necks); (*10*) Holocene cones with craters; (*11*) effusive domes; (*12*) volcanic cones with barrancos; (*13*) cliffs; (*14*) ridges of watersheds. (A–B–C) line of geological section.

part, while the older flows descend down for several kilometers in the south (Fig. 2). To the northeast from the Ivan Grozny Dome, the Drakon large extrusive dome rises. Acute lava tooths surround the remains of summit explosive crater, which ejected viscous lava flows to the south and north. The volume of Ivan Grozny volcano is 2.86 km^3, while Drakon volcano 1.08 km^3 (Bergal-Kuvikas, 2015).

Activity of Ivan Grozny Volcano in the Historical Time

Reliable and confirmed information on the activity of Ivan Grozny volcano in XVIII–XIX centuries was not found in the available historical overviews (Polonsky, 1994; Snow, 1992). First data on the volcanic activity could be attributed to the mid-XIX century: in the Japanese map of the Sakhalin-Kuril region of 1854 (Zharkov, 2014), the volcano is shown in the area of the present-day Grozny Ridge, with strong solfataras located in its summit and a thermal spring near its foot. According to the oral communication of Furukawa (Institute of Geology and Geoinformation, Geological Survey of Japan/AIST, Tsukuba, Japan)), this map likely demonstrates a long-term eruption of Ivan Grozny volcano, responsible for the formation of the extrusive dome.

Data obtained in summer 1951 point to an intensification of activity of Ivan Grozny volcano (Gorshkov, 1954). In particular, witnesses observed "flame," but later Gorshkov (1958) unambiguously attributed this activity to Baransky volcano. Indeed, local inhabitants told (Korsunskaya, 1958) that "fire" flashes and dark "smoke" were seen above the summit of Baransky volcano, while Ivan Grozny volcano in 1940–1950s, judging from descriptions and photos (Gorshkov, 1954, 1970; Korsunskaya, 1958), showed uninterrupted solfataric activity on the northern slope.

In 1964–1965, steam was observed near the northeastern foot of the dome, and the steam temperature in vents was no higher than 60°C (Abdurakhmanov et al., 1990). In July–August 1967, white steam jets were observed above the summit crater from the settlement of Burevestnik. In winter 1967–1968, these jets were clearly observed uninterruptedly. In February 1968, local inhabitants noted a 1–3 mm ash layer on snow, which had come from the volcano. In 1970, a weak ash emission was observed in the vicinity of the volcanic summit. From January 1971 to mid-May 1973, white gas jets were emitted from the northeastern side of the dome summit. On May 16, 1973, at 06:40 local time, a black ash-gas column ~600 m high rose above the volcano; in May 2017, resurgent ash fell on the northern slope of the volcano (Abdurakhmanov et al., 1990).

These events were followed by a long-term quiescence in the volcano activity. According to data of (Znamensky and Nikitina, 1985), the temperature of summit solfatara at the beginning of 1980s was much higher than 100°C. The temperature of associated solfataras reached 100°C. The summit solfatara mainly consisted of H_2S (63%) and CO_2 (28%). An airborne survey of the volcano by Sakhalin scientists in September 1988 noted its elevated solfataric activity (Abdurakhmanov et al., 1990).

The next eruption, described in detail in (Abdurakhmanov et al., 1990), began on May 3, 1989 with nearly constant emissions of steam-gas clouds, which with time transformed into an ash-gas column up to 2 km high. During the first emission, a new fissure was formed on the volcanic slope, then a summit fissure let forth two explosions. These activities were followed by explosions of different intensity, which have continued up to the end of August 1989. An explosion crater in the form of weakly steaming funnel ~30 m in diameter was formed in the upper part of the crater fissure; more intense solfataras were located below, along the crater fissure, as well as in the subsidiary tension cracks. The gas temperature in the mouth of one of the fumaroles reached 149°C. Steam-water jets with temperatures up to 100°C were noted downslope, on the continuation of the crater fissure. A new fissure formed on May 1989, which cut across the northern slope of the volcano, 100 m below the summit. It was 60–70 m long and 1–3 m wide, and the visible depth was around 40 m or more. The most powerful solfataric vents were confined to the floor of this new fissure. Deposits of resurgent ash reaching 20 cm thick were preserved around the fissure (Abdurakhmanov et al., 1990).

From 1989 to 2012, the main solfataric activity of Ivan Grozny volcano was confined to four areas (Zharkov, 2014; Semakin et al., 2000). The most powerful source of solfataric gases was located in the 1989 eruption fissure at an altitude of ~1120 m, and the second source was confined to the eastern flank of the deep explosive funnel. The third solfataric discharge site was confined to a small fissure located at the boundary of the northern block with dome slope (the northern fissure). The fourth vent was located to the northeast of the 1989 fissure eruption. From 1990 to 1998, temperature was measured in the most intense solfataras and gas samples were collected from Ivan Grozny volcano (Semakin et al., 2000). The determined maximum temperature of the most powerful solfataras of the 1989 fissure eruption reached 220°C (1990). Thereby, their gas composition was dominated by CO_2 (83.4% in dry gas) and H_2S (12.6%). In the next years, these solfataras had temperature within 157–197°C, and their composition was dominated by CO_2 (37–50% in dry gas), H_2S (10–40%), and SO_2 (7–49%), while HCl contents reached 0.7–28%, N_2, 2.2–9%. Other sites of solfatara discharge had similar gas composition, but temperatures within 100–160°C. After 1989 eruption, a thermal spring appeared on the southern coast of Lake Lopastnoe, near the northern foot of the dome. From 1990 to 1994, its temperature accounted for 28°C and then gradually increased, reaching 35°C in 1997 (Semakin et al., 2000).

Solfataras of Ivan Grozny dome and the Lopastnoy thermal spring were studied on September, 2004 (Zharkov, 2010, 2014). The temperature of solfataric vents in the eastern part of 1989 fissure, which formed a powerful steam-gas column, accounted for 95.5°C. The temperature of other solfataric vents on the volcano dome varied within 88–91.5°C. Several steam vents with temperature up to 40°C were found near the thermal spring; acid (pH 2.6) sulfate–chlorite sodium waters of the spring had a temperature of 41.5°C.

The next eruption of Ivan Grozny volcano began in mid-August 2012. The eruption was preceded by seismic activity from January to August 2012. The Kurilsk seismic station of the Sakhalin Branch of the Geophysical Survey RAS (Iturup Island) recorded dozens of seismic events directly beneath the Grozny volcanic ridge and to the south, in the Pacific Ocean. The strongest earthquakes with M = 4.3 with the epicenter on the southern slope of the volcano were recorded on August 6. At night, on August 16, a sharp gas smell was sensed in the town of Kurilsk and 1–2 mm of light gray ash fell; the ash also covered the summit of the Ivan Grozny dome. Explosions were also noted on August, 18–19, 21, 24, and 25 with a height of ash-

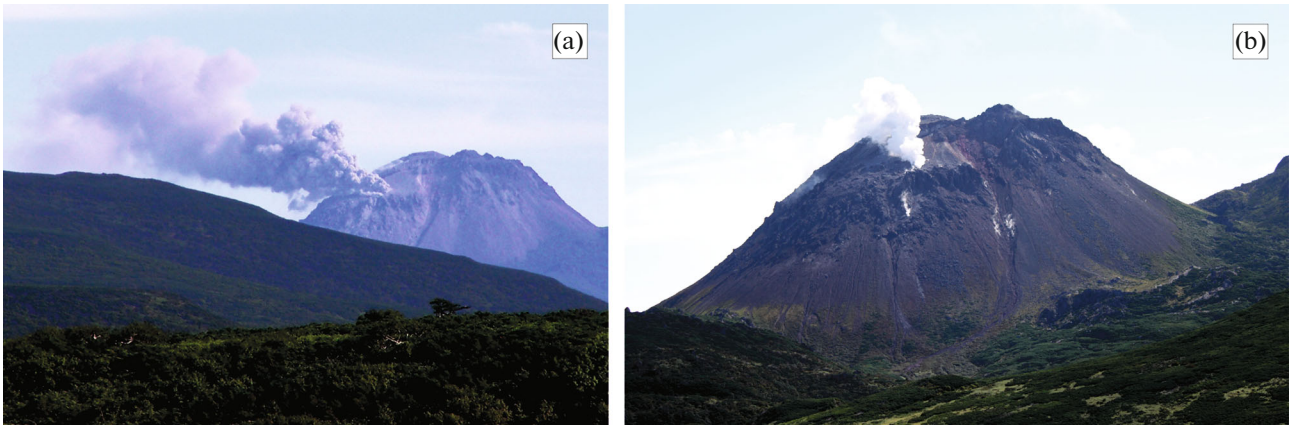

Fig. 4. Eruption of Ivan Grozny volcano in 2012: explosion on August 25, 2012 (a) (photo by R.V. Zharkov); explosion on August 28, 2012 (b) (photo by V.B. Guryanov).

gas column from 300 to 1200 m above the crater (Fig. 4a). At 20:04 on August 2026, an ash column was observed from the town of Kurilsk. It rose to a height of more than 2 km in a few minutes. According to data of the Kurilsk seismic station of the Sakhalin Branch of the Geological Survey RAS (Iturup I.), this explosion was preceded by an M = 3.9 earthquake with the epicenter 4 km northwest of the volcano. On August 28, geologists from the Institute of Marine Geology and Geophysics, Far Eastern Branch, Russian Academy of Sciences (IMGiG, FEB RAS) and town of South Sakhalinsk together, with EMERCOM and the department of the Civil Defense and Emergency Situations of the Kurilsk Urban District, flew a helicopter over Ivan Grozny volcano and took infrared, photo, and video records of the volcano and adjacent territory. Visually, the volcano did not change after several explosions; ash deposits were noted on the summit part of the dome, while the main source of steam-gas activity was confined to an altitude of ~1030 m (Fig. 4b). According to thermal imaging data (Zharkov and Kozlov, 2013), the temperature of steam-gas column accounted for 150–200°C. At 18:00, on August 29, a small ash emission occurred and a gray trail appeared over volcano, which with time was extended to Baransky volcano. The next explosion was recorded on September 28, at 16:30, an eruptive column around 1 km high was observed from Goryachie Klyuchi village. From October 2012 to March 2013, the volcano was characterized by elevated steam-gas activity; in a good weather, the residential inhabitants uninterruptedly observed a powerful steam-gas column. The last explosions were noted on April, 2013. In April 3, at 19:20, the eruptive column rose to a height over 2 km, and 2–3 mm of ash fell on the village of Goryachie Klyuchi and town of Kurilsk; on April 4, at 13:30, a short-term ash emission occurred at a height over 3 km, and the ash cloud moved in the northwestern direction (Zharkov, 2014; Zharkov and Kozlov, 2013).

During field work in August 2013 (Zharkov, 2014), the Ivan Grozny dome, as well as the Lopastnoy thermal spring, were studied. The physicochemical parameters of the thermal spring did not change significantly after the 2012–2013 eruption: weakly mineralized (M 1.2 g/dm^3), sulfate–chlorite sodium water with pH 2.05 had a temperature of 40°C. The 1989 eruption fissure on the dome summit did not experience significant changes, and the temperature of solfataric gases in the eastern part reached 90°C. Downslope, a northward open crater 60 × 80 m in size was formed on the site of the northern fissure at an altitude of ~1030 m (based on the GPS Garmin GPSMAP 62s data). Powerful steam-gas vents opened on the floor and steep walls of the crater; volcanic bombs up to 2–4 in size with fractured surface were found among ballistic blocks on the eastern edge of the crater (Fig. 5a). To the north of the dome, a single ballistic blocks thrown out for a distance up to 1.5 km from the eruption center were found; there were also small volcanic bombs with porous inner part and dense outer breadcrust-like parts (Fig. 5b). Near the northern foot of the dome, the buried snow is seen from beneath the clastic material of lahars, which indicates that lahars were formed by the explosion on April, 2013.

Composition of Igneous Rocks of Ivan Grozny Volcano

Data on the composition of modern igneous rocks of Ivan Grozny volcano in the scientific and archieved literature are scant. Only limited data on the chemical composition of ash of recent historical eruptions are available (Abdurakhmanov et al., 1990; Fedorchenko et al., 1989).

Ash from the 1973, 1989, and 2012–2013 eruptions are similar in chemical composition. On May 1973, resurgent ash of moderate-potassium andesite composition (SiO_2 59.23%, K_2O 0.91%) fell on the northern slope of Ivan Grozny volcano (Abdurakhmanov

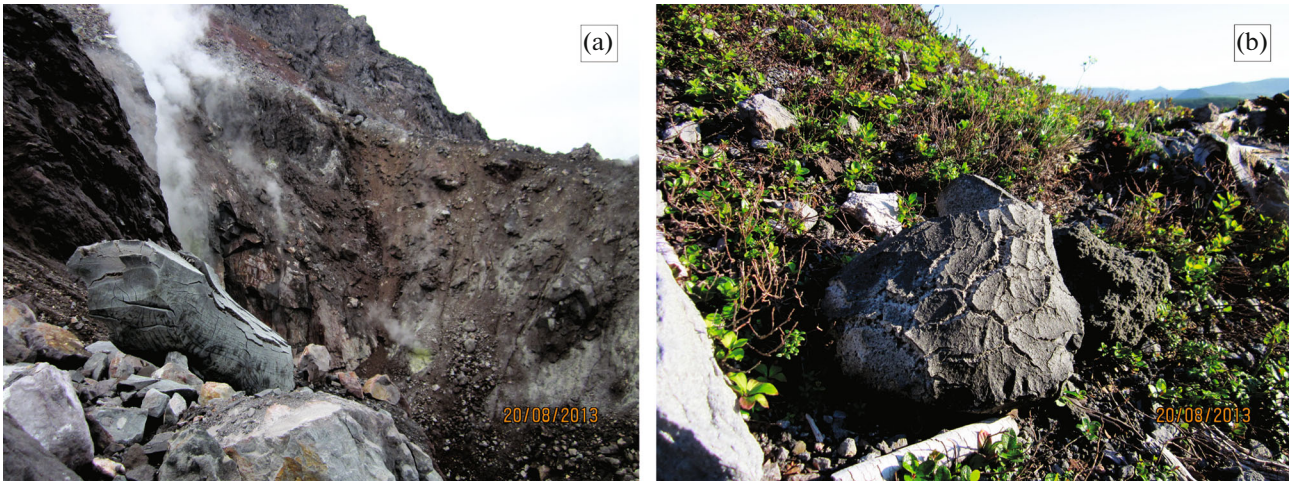

Fig. 5. Bombs and ballistic blocks on edge of crater of Ivan Grozny volcano (a) (photo by R.V. Zharkov); bomb on northern slope of Ivan Grozny volcano (b), sample 327 in Fig. 1d (photo by R.V. Zharkov).

et al., 1990) (Table 1). Ash that fell on May 1989 near the upper fissure of the extrusive dome has similar chemical composition, while ash collected near the lower fissure (Abdurakhmanov et al., 1990) had more acid composition and corresponds to dacitic andesites (SiO_2 63.00%) of moderate-potassium series (K_2O 0.94%) (Table 1).

On 2012, ash that fell in the area of the Okeanskaya GeoPPS, on the southwestern slope of Baransky volcano in composition (Table 1) corresponded to the andesite (SiO_2 – 57.20%) of the moderate-potassium series (K_2O – 1.03%). The grain-size composition was dominated by dust-size fraction <0.05 mm in size (38%); the coarse-grained particles over 0.25 mm across accounted for as low as 0.4%; the average ash mass along the ashfall axis accounted for 5.5 g/m^2 (Zharkov, 2014).

The ash of the 2013 eruption, which was collected on April 3 in Kurilsk, in addition to the fragments of the rocks of the old volcanic edifice, contained fresh volcanic glass, indicating an influx of a small amount of material from the upper part of the magma chamber (oral communication of A.V. Rybin, IMGiG FEB RAS). The selected samples were represented by light gray silty sands; the fraction washed from the 0.1–0.3 mm dust-size fraction consists of three components: fresh unaltered plagioclase, clinopyroxene, magnetite, and quartz; semitransparent fragments of groundmass with plagioclase microlites (around 80%), which is a typical mineral composition of andesites of the Ivan Grozny volcano dome; angular fragments of fresh transparent volcanic glass (up to 15%); hydrothermally altered rocks (greenish effusive rocks, cryptocrystalline light gray siliceous rocks, hematite) around 20%; the dusty part contains the same minerals, but dominated by fragments of transparent volcanic glass of angular shape. Ash of the 2013 eruption was studied only by optical methods, but we can state with confidence that they contain juvenile material and that the eruption of Ivan Grozny volcano is classified as phreatomagmatic.

In 2013, we sampled Late Pleistocene (?) lava flows, rocks of the volcano dome, and volcanic bombs of the 2012–2013 eruptions (Fig. 1d). The results of

Table 1. Chemical composition of ash from eruptions of Ivan Grozny volcano in 1973, 1989, and 2012 (wt %)

Sample	1	2	3	4
SiO_2	59.23	59.88	63.00	57.2
TiO_2	0.79	0.82	0.80	0.65
Al_2O_3	14.25	15.28	13.54	17.28
Fe_2O_3	3.67	2.62	3.45	7.41
FeO	4.33	6.91	4.52	
MnO	0.10	0.13	0.15	0.12
MgO	3.71	3.82	2.90	3.21
CaO	5.33	7.88	7.44	7.58
Na_2O	2.70	1.35	2.18	2.73
K_2O	0.91	0.48	0.94	1.03
P_2O_5	n.d.	0.08	0.09	0.08
H_2O	0.23	0.74	0.71	0.60
Total	100.21	100.11	99.82	97.89

(1) Ash that fell on May 17, 1973 (Abdurakhmanov et al., 1990); (2) ash that fell on May 8, 1989, near upper fissure (Abdurakhmanov et al., 1990); (3) ash that fell on May 8, 1989, near lower fissure (Abdurakhmanov et al., 1990); (4) ash that fell on August 18, 2012, in area of Okeanskaya geothermal power plant.

Table 2. Major oxides (wt %) and trace elements (ppm) of Ivan Grozny volcanic rocks collected in 2013

Sample	328	330	338	342	Crater-1	Crater-2	327	329
Sample type	Lava	Lava	Dome	Dome	Ash	Bomb	Bomb	Bomb
Age	Late Pleistocene	Late Pleistocene	Holocene	Holocene	2012–2013	2012–2013	2012–2013	2012–2013
XRF, %								
SiO_2	58.96	61.42	58.72	58.16	59.54	58.66	59.43	59.01
TiO_2	0.69	0.65	0.72	0.72	0.69	0.70	0.69	0.71
Al_2O_3	15.77	15.65	15.82	15.66	15.79	15.56	16.05	15.74
FeO	9.09	7.87	8.99	9.42	8.61	9.04	8.67	8.78
MnO	0.16	0.15	0.17	0.17	0.16	0.16	0.15	0.16
MgO	3.63	3.01	3.64	3.70	3.41	3.52	3.35	3.52
CaO	7.71	6.76	7.74	7.93	7.55	7.16	7.45	7.73
Na_2O	2.63	3.08	2.75	2.82	2.89	2.71	2.76	2.93
K_2O	0.93	1.14	0.96	0.96	1.03	0.95	1.02	1.05
P_2O_5	0.08	0.05	0.08	0.08	0.07	0.08	0.08	0.08
Total	99.65	99.78	99.59	99.62	99.74	98.54	99.65	99.71
ICP, ppm								
Be	0.69	0.81	0.76	0.07	0.54	0.13	0.55	0.48
Sc	18.3	20.4	25.1	25.8	20.8	27.3	12.9	24.2
V	231.0	206.0	268.0	246.0	225.0	255.0	201.0	254.0
Cr	31.5	18.0	24.1	24.8	26.4	25.1	22.7	44.9
Co	20.5	18.1	22.4	22.1	19.0	21.8	20.4	21.0
Ni	17.9	10.5	13.6	15.3	10.9	11.1	12.7	16.0
Cu	30.3	41.3	28.1	32.1	43.7	47.3	45.1	49.5
Zn	76.5	94.6	82.4	90.9	71.3	81.6	76.1	82.5
Ga	13.2	14.1	14.8	15.6	13.5	14.8	14.1	14.5
As	17.3	19.5	18.9	18.9	17.6	18.6	12.9	19.6
Rb	16.5	21.4	18.3	18.5	17.9	18.8	11.1	19.7
Sr	224.0	238.0	246.0	244.0	221.0	239.0	220.0	243.0
Y	20.9	22.1	23.0	22.4	20.8	22.4	19.6	24.2
Zr	78.8	98.3	84.8	85.6	81.3	87.2	83.8	90.9
Nb	0.99	1.13	0.91	0.91	0.91	0.97	0.04	1.18
Mo	2.14	2.21	1.83	2.19	2.11	2.92	0.98	3.59
Cd	0.14	0.24	0.03	0.09	0.03	0.15	0.02	0.10
Sn	2.78	9.25	2.70	2.84	2.81	3.02	2.72	2.94
Sb	0.34	5.66	0.39	0.33	0.28	0.31	0.08	0.37
Te	0.03	0.44	0.03	0.03	<0.01	0.07	0.11	0.07
Cs	1.17	1.27	1.34	1.36	1.30	1.06	0.62	1.43
Ba	191.0	256.0	213.0	203.0	214.0	216.0	179.0	232.0
La	4.60	4.78	5.14	4.88	5.06	5.44	4.61	5.52
Ce	11.6	12.6	13.1	12.7	13.2	14.2	11.9	16.4
Pr	1.67	1.76	1.85	1.80	1.79	1.89	1.81	1.95
Nd	7.90	8.03	8.90	8.20	8.59	8.62	8.25	9.36
Sm	2.41	2.34	2.49	2.54	2.45	2.63	2.54	2.84
Eu	0.69	0.58	0.51	0.65	0.78	0.53	0.58	0.82

Table 2. (Contd.)

Sample	328	330	338	342	Crater-1	Crater-2	327	329
Sample type	Lava	Lava	Dome	Dome	Ash	Bomb	Bomb	Bomb
Age	Late Pleistocene	Late Pleistocene	Holocene	Holocene	2012–2013	2012–2013	2012–2013	2012–2013
Gd	3.11	3.27	3.27	3.45	3.24	3.18	3.16	3.70
Tb	0.55	0.51	0.57	0.53	0.53	0.54	0.56	0.60
Dy	3.47	3.45	3.91	3.75	3.57	3.59	3.56	3.92
Ho	0.79	0.81	0.85	0.86	0.82	0.82	0.87	0.84
Er	2.27	2.59	2.59	2.56	2.34	2.36	2.41	2.53
Tm	0.36	0.38	0.40	0.39	0.35	0.40	0.34	0.39
Yb	2.28	2.58	2.70	2.48	2.32	2.57	2.56	2.66
Lu	0.35	0.45	0.42	0.42	0.40	0.41	0.39	0.43
Hf	2.36	3.14	2.41	2.66	2.51	2.59	2.38	2.75
Ta	0.08	0.09	0.10	0.07	0.07	0.07	0.11	0.09
W	0.45	0.59	0.51	0.52	0.69	0.77	0.08	0.70
Tl	0.15	0.06	0.11	0.11	0.12	0.17	0.11	0.16
Bi	0.09	0.11	0.07	0.05	0.06	0.15	0.03	0.08
Th	1.37	1.92	1.51	1.39	1.45	1.48	0.89	1.45
U	0.48	0.67	0.51	0.53	0.50	0.57	0.57	0.55

their chemical and microprobe analyses are presented in Tables 2 and 3.

The whole-rock chemical composition of analyzed magmatic rocks (Table 2) of Ivan Grozny volcano varies from andesites to dacitic andesites (SiO_2 = 58.16–61.42 wt %) with moderate K_2O contents (0.93–1.14 wt %) and low MgO (3.01–3.7 wt %). Slightly anomalous contents of some major and trace elements could be explained by the poorly representative collection of samples.

Variations of major oxides, in particular, the dependence of CaO and Al_2O_3 versus SiO_2 (Fig. 6, Tables 2, 3) observed in the volcanic glasses and in whole-rock sample of ash from Crater-1 indicate a crystallization differentiation and formation of rock-forming phenocrysts. Compared to the volcanoes from the rear zone (Bogdan Khmelnitsky volcano) and frontal zone (Baransky volcano) of Iturup Island, Ivan Grozny volcano has low ratios of incompatible elements (e.g., K_2O, Zr), which corresponds to the conditions of magma formation of the arc front. The dehydration of slab phlogopite beneath the rear part of the island arc, in contrast to the dehydration of amphibole and serpentine beneath frontal volcanoes, results in elevated contents of K, Rb, Ba, and Sr (Avdeiko et al., 1991). Based on the whole-rock composition and microprobe analyses of glasses, the differentiation trends of Pleistocene–Holocene rocks of Ivan Grozny volcano are represented by andesite–rhyolite series. Based on the Al_2O_3, K_2O, and MgO contents versus SiO_2, data points of samples do not define common trends, which are observed in the case of crystallization of main rock-forming minerals (Fig. 6). Obtained data indicate the complicated crystallization conditions and the heterogeneity of magmas on Ivan Grozny volcano. Periodic mixing of the magmas with cumulates was previously studied on Ivan Grozny volcano (Bindeman, 1997), where magmas varied from basaltic andesites to rhyodacites. It

Table 3. Microprobe measurements of volcanic glasses (wt %) in ash of 2012–2013 Ivan Grozny volcano eruption

Sample	Crater			
SiO_2	75.87	71.37	75.74	76.70
TiO_2	0.57	0.42	0.61	0.50
Al_2O_3	11.61	15.43	11.81	11.39
FeO	3.43	2.28	3.10	2.84
MnO	0.07	0.05	0.12	0.15
MgO	0.34	0.21	0.28	0.24
CaO	1.52	3.83	1.59	1.73
Na_2O	3.34	4.11	3.60	3.41
K_2O	3.16	2.18	3.07	2.87
P_2O_5	0.10	0.11	0.07	0.15

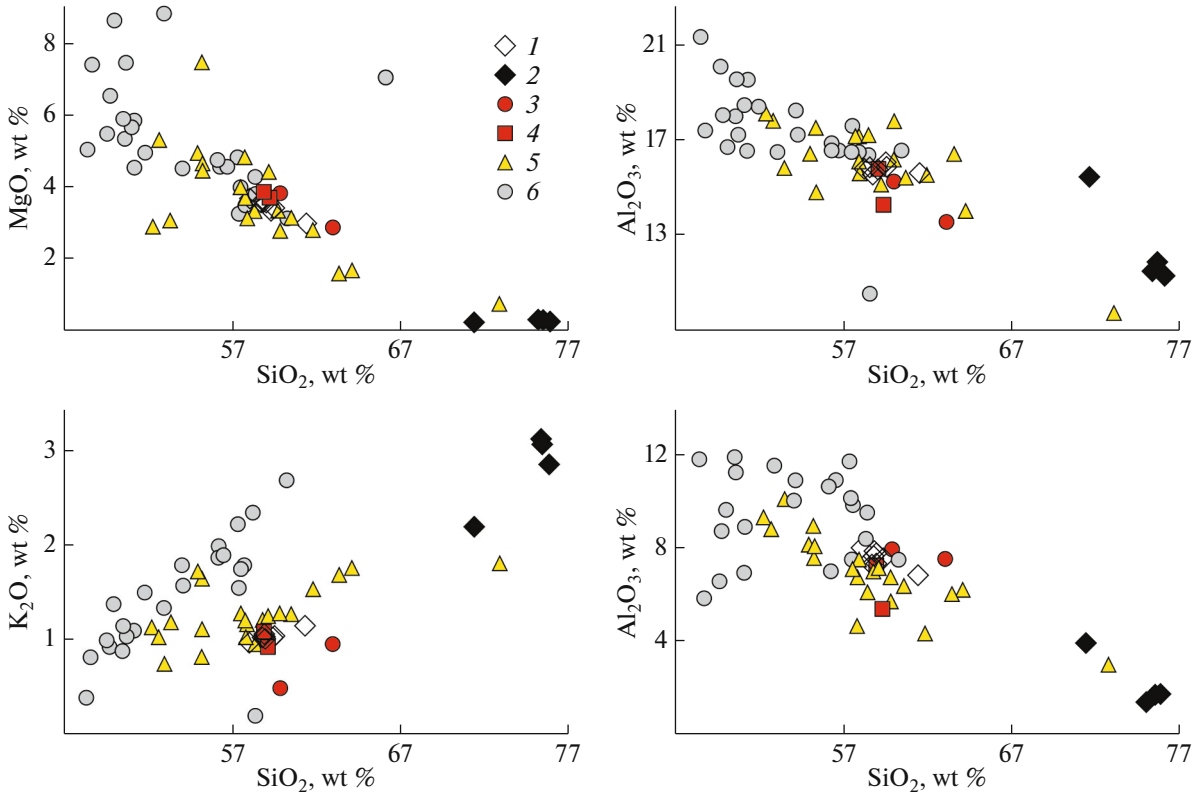

Fig. 6. Harker diagrams for Ivan Grozny volcano (white diamonds are data from whole-rock measurements; black diamonds are data from microprobe measurements of volcanic glass), Baransky volcano (yellow triangles are whole-rock compositions), Bogdan Khmelnitsky volcano (gray circles are whole-rock compositions). In addition, we used results of whole-rock measurements of lavas and ash of Ivan Grozny volcano from (Abdurakhmanov et al., 1990) (red circles); (Fedorchenko et al., 1989) (red squares). Data on Baransky and Bogdan Khmelnitsky volcanoes were collected from (Bindeman, 1997; Larin et al., 1996). Analytical measurements of samples are presented in Tables 2 and 3.

should be noted that the Ivan Grozny and Baransky volcanoes are situated in a similar geodynamic setting of the Grozny Ridge, which traces the frontal part of the Kuril Island Arc (Fig. 1).

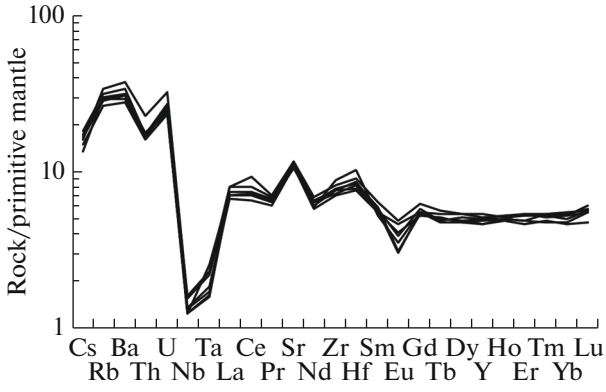

Fig. 7. Primitive mantle-normalized (Sun and McDonough, 1989) trace elements in samples from Ivan Grozny volcano. Trace element contents are presented in Table 2.

The distribution of trace elements (Fig. 7), in particular, the Nb–Ta minimum and relative Sr maximum observed in the spidergram, points to the typical subduction origin of magmas of Ivan Grozny volcano.

The results were compared with data on the mafic to felsic evolution of basaltic andesites to rhyodacites with heterogeneities in the compositions, structures, and inequilibrium combinations of phenocrysts in lavas of Baransky volcano (Bindeman, 1997). The close position of the active Baransky and Ivan Grozny volcanoes in the frontal part of the arc and scarce explosions with the predominance of resurgent material make it impossible to correlate distal ash from these sources using only the whole-rock major oxide composition. The data in terms of relations of incompatible elements, including K_2O (Fig. 6) and Rb, Zr, Sr, and Ba (Fig. 8), clearly show differences in variations of the magma of the Baransky and Ivan Grozny volcanoes in the frontal zone, which suggests different conditions of fractionation and magma assimilation in the crust. At the same time, Bogdan Khmelnitsky volcano demonstrates approximately similar increase of incompatible elements, including Zr and Rb (Fig. 8),

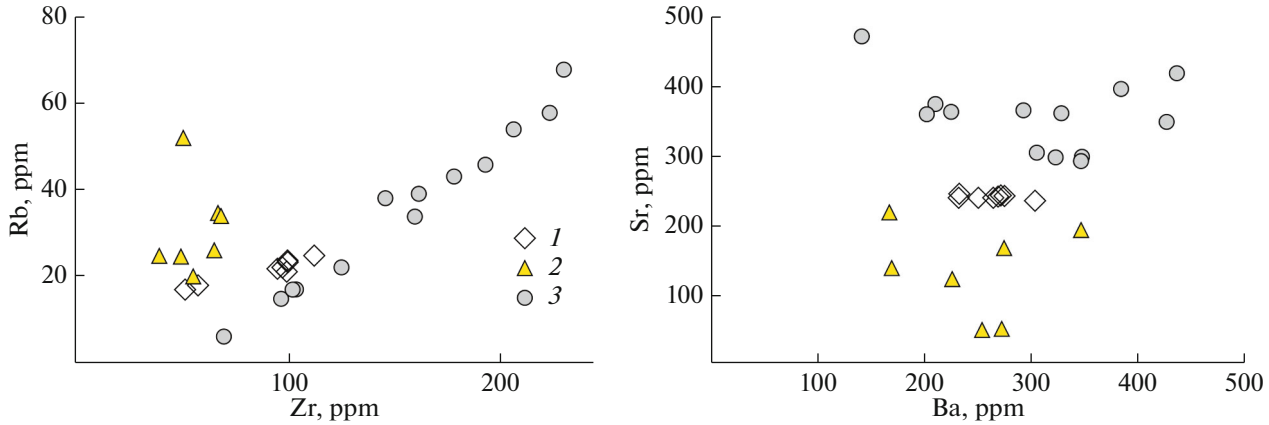

Fig. 8. Relations of incompatible elements in whole-rock compositions of samples from Ivan Grozny volcano (white diamonds), Baransky volcano (yellow triangles), and Bogdan Khmelnitsky volcano (gray circles). Data on Baransky volcano and Bogdan Khmelnitsky volcano from publications (Bindeman, 1997; Larin et al., 1996) are shown for comparison. Analytical measurements of samples are presented in Table 2. Note: Zr content was not determined in some compared samples.

which is consistent with the classical scheme of fractional differentiation of magmas. Ivan Grozny volcano is characterized by an increase in Rb content with increasing Zr and a decrease of Sr content with increasing Ba; Baransky volcano, in contrast, shows no such variations. Thus, the Rb/Zr and Sr/Ba ratios could be used as peculiar characteristics for correlating the distal ashes of eruptions of given volcanoes.

Assessment of Volcanic Hazard of Explosive Eruptions of Ivan Grozny Volcano

After the 2012–2013 eruptions, Ivan Grozny volcano transformed to the stationary stage of solfataric activity. Already by 2014, only insignificant steam-gas emissions from the 1989 fissure and newly formed crater were seen visually from the town of Kurilsk and Oceanskaya GeoPPS. In subsequent years, the intensity of steam-gas activity decreased, judging from the visual observations and Sentinel-2 satellite images during 2017–2023, and became minimal by the present day. In spite of the visible decrease in steam-gas activity, the volcano could erupt at any moment. Depending on the type of eruption and power, the negative consequences will span the central part of Iturup Island, which comprises all infrastructural objects and settlements inhabited by approximately 7000 humans (January 1, 2023. https://sakhalin.gov.ru/index.php?id=678).

The hazard for active volcanoes of the Kuril–Kamchatka island-arc system is traditionally estimated by considering the following hazardous processes and phenomena: lava flows, lahars, pyroclastic flows and waves, avalanche/avalanche–explosive phenomena, and ashfalls (Bazanova et al., 2001; Girina et al., 2018; Gordeev et al., 2016; Melekestsev et al., 1987; Ozerov et al., 2020; Rybin et al., 2017; Chibisova et al., 2023). Most of the aforementioned phenomena are not typical of the modern activity of Ivan Grozny volcano (Abdurakhmanov et al., 1990; Zharkov, 2014) and could have a destructive effect within a radius of several kilometers from the volcano, where there are no settlements or infrastructural objects. Therefore, in this study, we only assess hazard related to ashfall, since ashfalls are the most frequent manifestations of active volcanic activity on the Kuril Islands. The spread of ashfall depends on the power of explosions, wind direction, and speed in the eruption zone, and the general circulation of air masses, which control ash transport for thousands of kilometers. Iturup Island is characterized by the seasonal change in wind direction related to cyclonic activity (*Atlas...,* 2009): the north-

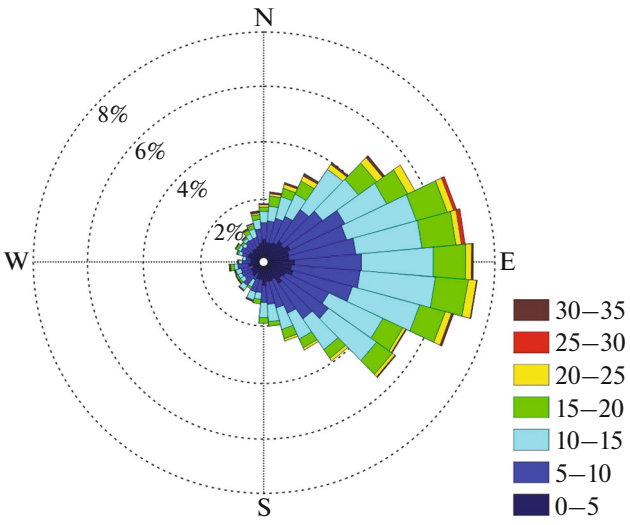

Fig. 9. Seasonal wind directions in area of Ivan Grozny volcano for emission heights of 0–5 km above sea level over all seasons (Mastin, 2017). Color symbols on right shows wind speed in m/s.

erly and northwesterly winds predominate during the cold period (October–April), whereas southeasterly winds are typical of the warm period. According to the meteorological database (Mastin, 2017), southeasterly, easterly, and northeasterly winds predominate in the vicinity Ivan Grozny volcano up to a height of 5 km above sea level throughout the year (Fig. 9). Therefore, during explosive eruptions with a small height of eruptive clouds typical of the volcano (Abdurakhmanov et al., 1990; Zharkov, 2014), ash flows will propagate mainly to the northwest, west, and southwest. Given that the main infrastructural objects and settlements of the island, including the district center (the Kurilsk) are located to the north and west of Ivan Grozny volcano (24 km north of the volcano, the population as of January 1, 2023, was 2537, according to data https://sakhalin.gov.ru/index.php?id=678), negative economic and social consequences from explosive eruptions are possible. A similar wind regime and, respectively, directions of ash flow propagation are typical of all seasons and emission heights up to 24 km above sea level. Above this level, northwesterly and northeasterly winds predominate in the cold period, while the warm period is characterized by westerly winds (Mastin, 2017). Therefore powerful ultra-Plinian eruptions (VEI 5 and more) with an emission height of 24–40 km above sea level (in historical time, eruptions with VE5 or more were not recorded in the Kuril Islands; in this study, shown for comparison) and transport of ash flows to the east could represent a hazard for international airlines passing along the Kuril Islands, 80–150 km from volcano.

In general, the presented theoretical calculations of the propagation of ash flows of Ivan Grozny volcano were confirmed by the visual observations and satellite data in 2012–2013 (Zharkov, 2014). Therefore, it should be taken into account that in a real situation, the propagation of ash flows is governed by cyclones and typhoons, which significantly modify the local meteorological conditions.

CONCLUSIONS

This article studied the active Ivan Grozny volcano, the last explosive eruption of which was observed in 2012–2013. The whole-rock composition of volcanic products determined by modern analytical methods for edifice and pyroclastic samples varies from andesites to dacitic andesites (57.20–61.42 wt % SiO_2) of the moderate-potassium series (0.93–1.14 wt % K_2O) with a low Mg# (<5 wt % MgO). The microprobe studies of volcanic glasses in 2012–2013 eruption products yielded the following composition: 71.37–76.7 wt % SiO_2, 2.18–3.16 wt % K_2O, 0.21–0.34 wt % MgO. Compared to the volcanoes of the rear (Bogdan Khmelnitsky volcano) and frontal (Baransky volcano) zones of Iturup Island, the rocks of Ivan Grozny volcano are characterized by low contents of incompatible elements (e.g., K_2O, Zr), which corresponds to the conditions of magma formation in the frontal arc. The distribution of trace elements indicates a typical subduction origin of magmas. The rocks of the volcano are characterized by an elevated Rb content with increasing Zr and a decrease in Sr content with increasing Ba.

Relatively weak explosive eruptions typical of Ivan Grozny volcano in historical time represent a hazard for settlements and infrastructural objects of Iturup Island, because ash flows will be transported to the northwest, west, and southwest of volcano, toward the most populated and economically developed area of Iturup Island. Powerful eruptions with an emission height over 24 km could result in catastrophic consequences for international airlines flying from North America to Asia along the Kuril Islands.

ACKNOWLEDGMENTS

The authors thank colleagues that participated in field studies, analytical studies, and discussion of the results, as well as the anonymous reviewers and editorial staff of the journal, whose constructive criticism and comments allowed us to significantly improve the text.

FUNDING

Measurements of major oxides and trace elements were supported by the Russian Science Foundation, project no. 21-17-00049, https://rscf.ru/project/21-17-00049.

CONFLICT OF INTEREST

The authors of this work declare that they have no conflicts of interest.

REFERENCES

A. I. Abdurakhmanov, T. K. Zlobin, E. K. Markhinin, and R. Z. Tarakanov, "The Ivan Groznyi volcano eruption on Iturup Island in 1989," Vulkanol. Seismol., No. 4, 3–9 (1990).

Atlas of the Kuril Islands, Ed. by N. N. Komedchikova (DIK, Moscow–Vladivostok, 2009).

G. P. Avdeiko, O. N. Volynets, A. Yu. Antonov, and A. A. Tsvetkov, "Kurile island-arc volcanism: structural and petrological aspects," Tectonophysics **2** (4), 271–287 (1991). https://doi.org/10.1016/0040-1951(91)90175-R

L. I. Bazanova, O. A. Braytseva, I. V. Melekestsev, and M. Yu. Puzankov, "Potential hazards from the Avachinsky volcano eruptions," *Geodynamics and Volcanism of the Kuril–Kamchatka Island-Arc System* (IVGiG DVO RAN, Petropavlovsk-Kamchatskiy, 2001), pp. 390–407.

O. V. Bergal'-Kuvikas, "Volumes of Quaternary volcanic material of the Kuril Island Arc: analysis of spatial variations in correlation with subduction zone," Tikhookean. Geol. **34** (2), 103–116 (2015).

I. N. Bindeman, "Magma and cumulate mixing as a mechanism of the cyclic evolution of Baranskogo Volcano, Iturup, Kuril Islands," Geochem. Int. **35** (4), 329–338 (1997).

Ya. V. Bychkova, M. Yu. Sinitsyn, D. B. Petrenko, et al., "Method peculiarities of multielemental analysis of rocks with inductively-coupled plasma mass spectrometry," Moscow Univ. Geol. Bull. **72** (1), 56–62 (2016).

M. V. Chibisova, A. V. Degterev, A. V. Rybin, and F. A. Romanyuk, "Sakhalin Volcanic Eruption Response Team (SVERT): 20 years of monitoring of volcanic activity on the Kuril Islands," Geosist. Perekhod. Zon **7** (4), 448–453 (2023).

V. I. Fedorchenko, A. I. Abdurakhmanov, and R. I. Rodionova, *Volcanism of the Kuril Island Arc: Geology and Petrogenesis* (Nauka, Moscow, 1989).

S. D. Gal'cev-Bezyuk, *Toponymical Glossary of the Sakhalin Region* (Dal'nevost. Knizh. Izd-vo, Sahalinskoe otd., Yuzhno-Sahalinsk, 1992). O. A. Girina, E. A. Lupyan, A. A. Sorokin, et al., Comprehensive monitoring of explosive volcanic eruptions of Kamchatka. (IViS DVO RAN, Petropavlovsk-Kamchatskiy, 2018).

E. I. Gordeyev, O. A. Girina, E. A. Lupyan, et al., "The VolSatView information system for monitoring the volcanic activity in Kamchatka and on the Kuril Islands," J. Volcanol. Seismol. **10** (6), 382–394 (2016). https://doi.org/10.1134/S074204631606004X]

G. S. Gorshkov, "Chronology of volcanic eruptions of the Kuril Ridge (1713–1952)," Tr. Lab. Vulkanol. **8**, 58–99 (1954).

G. S. Gorshkov, "Active volcanoes of the Kuril island arc," Tr. Lab. Vulkanol. **13**, 5–70 (1958).

G. S. Gorshkov, *Volcanism and the Upper Mantle: Investigations in the Kurile Island Arc* (Plenum Press, New York–London, 1970).

A. Harker, *The Natural History of Igneous Rocks* (Methuen & Co, London, 1909).

E. Kalnay, M. Kanamitsu, R. Kistler et al. "The NCEP/NCAR 40-Year Reanalysis Project," Bull. Am. Meteorol. Soc. **77** (3), 437–471 (1996). https://doi.org/10.1175/1520-0477(1996)077<0437:TNYRP>2.0.CO;2

G. V. Korsunskaya, *Kuril Island Arc* (Physico-Geographical Overview (Gos. Izd-vo Geograf. Lit., 1958).

N. V. Larin, I. N. Bindeman, and A. G. Simakin, "Petrology of Bogdan Khmelnitsky volcano on Iturup Island, Kurils: a model of fractional differentiation and mixing in a magma chamber," Vulkanol. Seismol., No. 5, 28–41 (1996).

L. G. Mastin, *Plots of Wind Patterns of the World's Volcanoes,* U.S. Geol. Surv. Data Release (2017). https://doi.org/10.5066/F7SQ8XKT

I. V. Melekestsev, O. A. Braytseva, and V. V. Ponomareva, Dynamics of activity of the Mutnovsky and Gorely volcanoes in the Holocene and volcanic hazard to the surrounding areas (according to tephrochronological data)," Vulkanol. Seismol., No. 3, 3–18 (1987).

Method of Quantitative Chemical Analysis. Determination of Fluorine, Sodium, Magnesium, Aluminum, Silicon, Phosphorus, Potassium, Calcium. Scandium, Titanium, Vanadium, Chromium, Manganese, Iron, Cobalt, Nickel, Zircon, and Niobium in Rocks, Ores, and Products of their Processing by X-ray Spectral Fluorescence Method. (Method NSAM no. 439-RS). Industrial Technique of the 3rd Accuracy Category (VIMS, Moscow, 2010).

Method of Quantitative Chemical Analysis. Determination of Trace Elements in Samples: Be, Mg, Al, Si, Ca, Sc, Ti, V, Cr, Mn, Fe, Co, Ni, Cu, Zn, Ga, As, Se, Sr, Y, Zr, Nb, Mo, Pd, Ag, Cd, In, Sn, Sb, Te, Ba, La i drugikh RZE, Hf, Ta, W, Re, Os, Pb, Th, and U, as well as in samples of their oxides and salts by ICP-MS (Technique NSAM No. 501-MS). Industrial Technique of the 3rd Accuracy Category (VIMS, Moscow, 2011). .

A. Y. Ozerov, O. A. Girina, N. A. Zharinov, et al., "Eruptions in the northern group of volcanoes, in Kamchatka, during the early 21st Century," J. Volcanol. Seismol. **14** (1), 1–17 (2020). https://doi.org/10.1134/S0742046320010054]

A. S. Polonskiy, "Kuriles," Krayeved. Byull. Yuzhno-Sakhalinska, 3 (1994).

A. V. Rybin, M. V. Chibisova, A. V. Degterev, and V. B. Gur'yanov, "Volcanic eruptions in the Kuril Islands during 21st century," Vestn. DVO RAS, No. 1, 51–61 (2017).

L. Siebert, T. Simkin, and P. Kimberly, *Volcanoes of the World* (University of California Press, Berkeley, 2010).

H. Snow, Notes about the Kuril Islands, Krayeved. Byull. Yuzhno-Sakhalinsk, No. 1, 89–127 (1992).

S. S. Sun and W. F. McDonough, "Chemical and isotopic systematics of oceanic basalts: implications for mantle composition and processes," Geol. Soc. Spec. Publ. **42**, 313–345 (1989). https://doi.org/10.1144/GSL.SP.1989.042.01.19

R. V. Zharkov, "Modern solfataric-hydrothermal activity of volcanoes of the Grozny Ridge (Iturup, Kuril Islands)," *Proc. IVth Sakhalin Youth School "Natural Catastrophes: Study, Monitoring, and Prediction,* (IMGiG DVO RAN, Yuzhno-Sakhalinsk, 2010), pp. 191–197.

R. V. Zharkov, "Volcanic landforms of the Grozny Ridge (Iturup Island, Kuril Islands)," *Proc. 23rd Plenum of the Geomorphological Commission of RAS "Geomorphology and Cartography* (SarGU, Saratov, 2013), pp. 383–386.

R. V. Zharkov, Thermal Springs of the South Kuril Islands (Dal'nauka, Vladivostok, 2014).

R. V. Zharkov and D. N. Kozlov, "Explosive eruption of Ivan Grozny volcano in 2012–2013 (the Iturup Island of the Kurile Islands)," Vestn. DVO RAS, No. 3, 39–43 (2013).

V. S. Znamenskiy and I. B. Nikitina, "Hydrothermal vents of the central part of Iturup Island (Kuril Islands)," Vulkanol. Seismol., No. 5, 44–65 (1985).

Translated by M. Bogina